ISSN 0967-0912, Steel in Translation, 2022, Vol. 52, No. 9, pp. 844–851. © Allerton Press, Inc., 2022.
Russian Text © The Author(s), 2022, published in Izvestiya Vysshikh Uchebnykh Zavedenii, Chernaya Metallurgiya, 2022, No. 9, pp. 644–653.

Features of Microstructure, Phase Composition and Strengthening Capability of Stainless Steels with Chromium Content of 13–17%

D. A. Pumpyanskii[a, *], I. Yu. Pyshmintsev[b], S. M. Bityukov[c, **], M. A. Gervas'ev[a], and A. A. Gusev[b, *]**

[a] *B.N. Yeltsin Ural Federal University, Yekaterinburg, 620002 Russia*
[b] *OOO TMK STC, Skolkovo, Moscow, 143026 Russia*
[c] *OAO Russian Scientific Research Institute of the Pipe Industry, Chelyabinsk, 454139 Russia*
**e-mail: pyshmintseviu@rosniti.ru*
***e-mail: secretariat@rosniti.ru*
****e-mail: GusevAA1@tmk-group.com*

Received April 26, 2022; revised August 22, 2022; accepted August 26, 2022

Abstract—The paper studies features of structural and phase transformations of complex alloyed high-strength martensitic, austenitic-martensitic and martensitic-ferritic steels that are resistant to carbon dioxide corrosion and have a chromium content of 13–17%. The influence of the alloying system on the crystallization and phase transformations at hot strain and thermal treatment temperatures is studied by thermodynamic modeling and experiment. The effect of the quenching temperature on the phase composition and microstructure of the steels is analyzed by the results of X-ray diffraction phase analysis and optical and transmission electron microscopy. It is found that, with an increase in the nickel content, a lot of austenite is retained in the metal microstructure, which significantly decreases the creep limit at high tensile strength and ductility. To obtain a predominantly martensitic microstructure in the martensitic-austenitic steel with a chromium content of 15%, the multistage heat treatment is proposed. This treatment includes quenching, intermediate annealing for the precipitation of dispersed carbide particles, the composition of which is estimated by X-ray microanalysis, and tempering intended to shape the final mechanical properties of steel. According to the results of the elongation tests of martensitic and martensitic ferrite steels, their necessary strengths ($\sigma_{0.65} \geq 862$ MPa; $\sigma_u \geq 931$ MPa) are reached after the heat treatment by quenching and tempering. The required strength properties of the steel with a large fraction of nickel and chromium content of 15% are ensured by multistage heat treatment, including quenching, intermediate annealing and final tempering.

Keywords: high-chromium steels, two-phase structure, heat treatment, transmission electron microscopy, X-ray microanalysis, secondary phase, lath martensite, retained austenite, δ ferrite

DOI: 10.3103/S0967091222090091

INTRODUCTION

The interest in high-strength corrosion resistant steels with a high chromium content has risen progressively as deep wells (more than 4000 m) have been developed for producing oil and gas with carbon dioxide in their products.

The development of new steel compositions for making casing and tubing is intended to maintain high corrosion resistance during the operation at temperatures of 200°C and under a partial carbon dioxide pressure of 10 mPa over Cl^- ions [1–3]. In such conditions, the application of 13Cr is limited by insufficient corrosion resistance and the application of 22Cr and 25Cr steels is limited by high production costs and narrow range of pipe products. Considering the above indicated requirements, martensitic and transitional steels with a Cr content of 15–17% enjoy an ever widening application. High strength and good machinability have allowed using these steels as high-load steels in a lot of industries, such as airspace and oil chemical industry, and also on nuclear power engineering and marine engineering facilities [1, 4–7].

To form an optimal microstructure and ensure a required mechanical performance level, it is necessary to understand the influence of chromium and nickel on phase transformation patterns. This will prevent the generation of δ ferrite and austenitic residues though retain a mainly martensitic structure [8–11].

To enhance the set of their mechanical properties, local corrosion resistance, and hinder the austenitic grain growth at heating, the molybdenum content in

Table 1. Chemical composition of the test steels, wt %

Composition	C	Si	Mn	S	P	Cr	Ni	Mo	Cu	W
1	0.04	0.31	0.33	0.003	0.007	13.2	5.1	2.1	0.025	0.01
2	0.08	0.37	0.42	0.005	0.007	15.2	6.5	2.2	0.024	0.01
3	0.08	0.29	0.44	0.004	0.010	17.2	3.9	2.6	0.900	1.00

the steels of this class must be up to 3% [8, 9, 11, 12]. Sometimes, steel is alloyed with tungsten for partially replacing molybdenum, enhance the mechanical properties of steel and reduce its temper brittleness [13–15].

The additional alloying of such steels with copper was used for dispersion hardening by analogy with steels used in the airspace sector and other fields [9, 12–15]. The enhancement of the creep limit at the release of ε-Cu particles from martensite depends on the degree of its oversaturation with copper and the development of parallel tempering processes involving carbide-forming elements such as chromium, molybdenum and tungsten.

The goal of this work is to study the features of phase transformation of complex alloyed steels with a Cr content of 13–17% for choosing a rational composition ensuring improved performance properties.

MATERIALS AND METHODS

The materials chosen for the study were three steels which differed in the content of chromium as the main element determining their corrosion resistance and the ratio of ferrite-forming and austenite-forming elements. The smelting was carried out in a laboratory vacuum induction furnace. The ingots were heated to 1180–1200°C in a through-type furnace with homogenizing soaking.

The ingots were hot-rolled into bars of 16 mm in diameter in three steps at a final rolling temperature of not less than 850°C. After the rolling, the bars were cooled in smooth air to the shop temperature and then heat-treated in high tempering mode at 620°C with a soaking for 1 h. The chemical composition of the test compositions is given in Table 1.

The temperatures of critical points of the test steels were measured dilatometrically and by calculation using the Thermo-Calc software [16]. The phase composition of the steels was studied by X-ray structural phase analysis on a D8 ADVANCE diffraction meter with a cobalt anode.

The microstructure of the steel was examined with the help of an optical inverted microscope Axio VertA1 MAT (with etching in Marble's reagent) and a JEOL JEM-2100 Plus transmission electron microscope (TEM). The chemical composition of secondary phases was determined using a Bruker energy dispersive spectrometer integrated with the TEM. The foil for the tests under the TEM was prepared from blanks with a thickness of 0.5 mm and mechanical thinning to 0.05–0.10 mm and electrolytic etching at –20°C in a solution containing 430 mL of H_3PO_4, 25 mL of H_2SO_4 and 50 g of CrO_3.

The tensile strength and plastic properties were determined according to GOST 1497 on cylindrical specimens with their working section diameter of 5 mm on a universal testing machine MTS Insight.

RESEARCH RESULTS

The values of critical points determined by the dilatometric method are shown in Table 2. The specimens were heated to a temperature of 920°C at a rate of 610°C/h. The heating mode was closest to the production conditions. The initial temperature of martensitic transformation was determined on cooling the samples in calm air. The average rate of cooling from 920°C to room temperature was 12 500°C/h.

For composition 1 and 2 steels the respective temperature of point As_1 is 590 and 615°C, which limits the tempering temperature that does not lead to the formation of austenite. Composition 2 steel has the lowest initial temperature of martensitic transformation, which leads to a large amount of residual austenite after quenching and generation of a two-phase austenitic martensitic structure.

The modeling of phase transformations at thermodynamic equilibrium showed that there were several kinds of these characteristics for the test steels (Fig. 1):

— crystallization with the generation of only δ ferrite that remains stable in a narrow temperature range and completely converts to austenite at further cooling (composition 1 steel, Fig. 1a);

— peritectic crystallization with the complete transformation of δ ferrite at cooling to austenite that remains stable in a broad temperature range (composition 2 steel, Fig. 1b);

Table 2. Temperatures of critical points of the steels

Composition	Critical point temperatures, °C		
	As_1	As_3	M_s
1	590	717	182
2	615	702	57
3	673	726	156

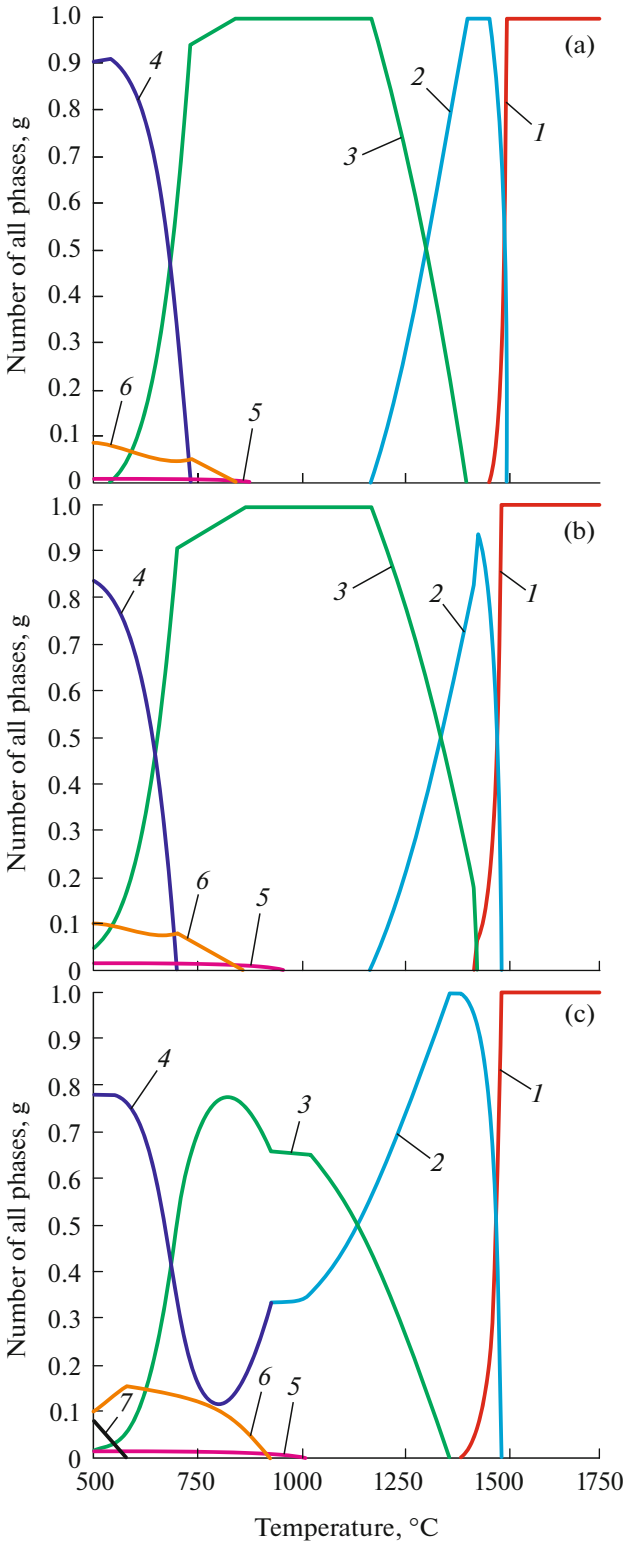

Fig. 1. Phase composition of the test steels at thermodynamic equilibrium and temperatures from 1500 to 500°C: (a) composition 1 steel; (b) composition 2 steel; (c) composition 3 steel; (*1*) the melt; (*2*) the δ ferrite; (*3*) the γ phase; (*4*) the α phase; (*5*) $Me_{23}C_6$ carbide; (*6*, *7*) the σ phase.

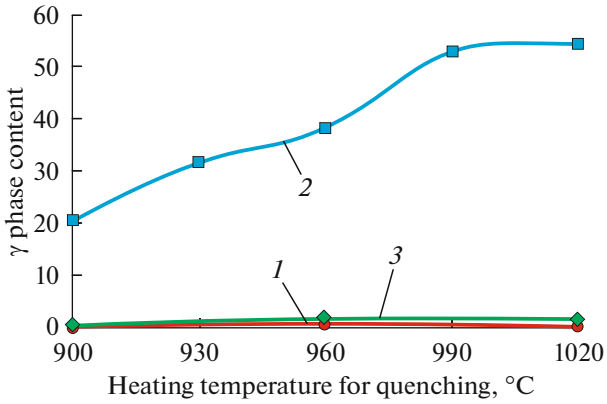

Fig. 2. Influence of the heating temperature for quenching on the γ phase content in the steels with compositions 1—3.

— crystallization with the formation of only δ ferrite, which converts mostly to austenite at subsequent cooling. In this case, about 30% of δ ferrite is retained at temperatures of 915–1020°C; however, at 805–915°C the amount of δ ferrite decreases to 10–15% due to the release of carbide and σ phase (composition 3 steel, Fig. 1c).

The transition from composition 1 martensitic steel to composition 2 and 3 steel, that is associated with an increase in the content of carbide-forming elements, increases the initial temperature of the release of secondary phases, including σ phase and $Me_{23}C_6$ carbides. The release of σ phase in the practical heat treatment of the test steels does not usually occur due to relatively short dwell times.

Considering the dilatometry and modeling results, the effect of the quenching temperature for heating on the phase composition and microstructure was studied by experimentation at temperatures from 900 to 1020°C.

The amount of γ phase residues at room temperature was determined by X-ray phase analysis after quenching from the above temperatures (Fig. 2). According to the quenching results, the test steels are divided into two groups:

— steels 1 and 3 with no more than 2% of residual austenite;

— steel 2 with a large amount of residual austenite.

After quenching from 960 to 1020°C, composition 1 steel has a lath martensite structure; depending on the heating temperature, the initial austenite grain size varies from 20 to 50 μm. After quenching from 1020°C, composition 2 steel has a coarse-grained structure with batch martensite (Fig. 3a) and up to 55% of residual austenite (Fig. 3b).

Quenched composition 3 steel has a two-phase structure of martensite and δ ferrite (Fig. 4). The increase in the heating temperature for quenching from 960°C (Fig. 4a) to 1020°C (Fig. 4b) is accompa-

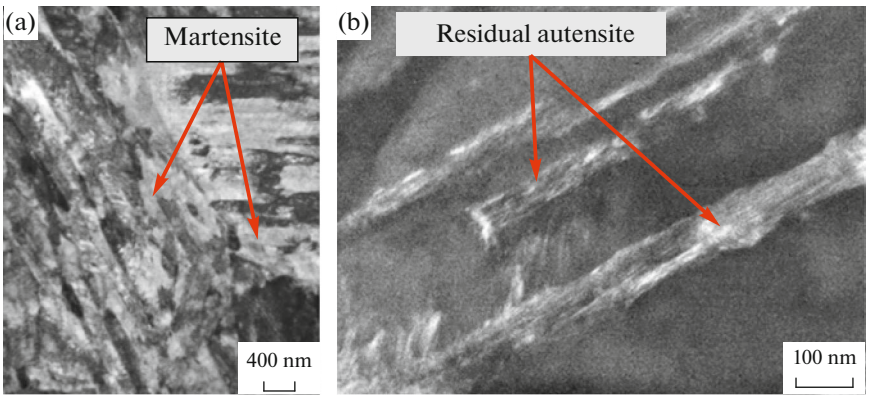

Fig. 3. Bright-field (a) and dark-field (b) images of microstructure of steel 2 after quenching at 1020°C.

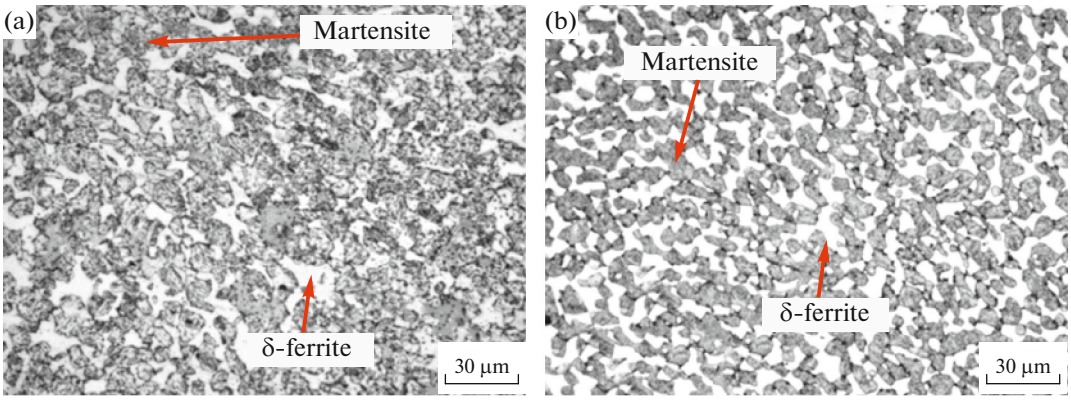

Fig. 4. Microstructure of steel 3 after quenching at temperatures of 960 (a) and 1020°C (b)

nied by the growth of the fraction of δ ferrite in the structure of steel from 20 to 30%.

The test steels were quenched from 960°C and then tempered at temperatures from 530 to 590°C.

In the whole range of tempering temperatures, martensitic and martensitic ferritic steels have high creep limits and tensile strengths (Fig. 5a). The highest rupture strength of at least 1080 mPa is shown by composition 2 transitional austenitic martensitic steels. However, the high fraction of residual austenite results in a low creep limit in the whole range of tempering temperatures. The relative elongation, the test steels retained in this range varied from 18 to 22%, which indicated that they had a sufficiently high ductility. Thus, the ultimate thermal treatment of composition 2 steel by quenching from 960°C with one-off tempering does not allow producing a homogeneous martensitic structure ensuring high creep limit levels. This is why, to produce a predominantly martensitic structure, the ultimate thermal treatment of composition 2 steel was conducted by quenching from 1020°C followed by 2-h annealing at 760°C and final 1-h tempering at 530°C.

The choice of a high heating temperature for quenching was aimed at dissolving the large amount of carbide phase and evenly distributing the alloying elements in the solid solution [9, 17–20].

The annealing at temperatures above point As_3 (760°C) leads to the release of carbide phases from austenite, which depletes it in the content of carbon and alloying elements and makes it less stable, also resulting in a higher initial temperature of martensitic transformation (point M_n). The subsequent air cooling to room temperature is accompanied by the formation of martensite with the preservation of the released carbide phases. According to the X-ray structural phase analysis, the amount of austenite residues in composition 2 steel after annealing decreased to 10%.

The microstructure of the annealed steel of this composition consists from almost rectangular packages of *fresh* (newly formed) martensite, located on the place of the former austenite grain (Fig. 6a), as well as carbide phase particles separated from austenite during the annealing (Fig. 6b). The carbides not exceeding 150 nm in size are mainly located along the boundaries of the former austenitic grain and are elongated or almost globular in shape.

According to the X-ray microspectral analysis, in the annealed composition 2 steel, carbides have an

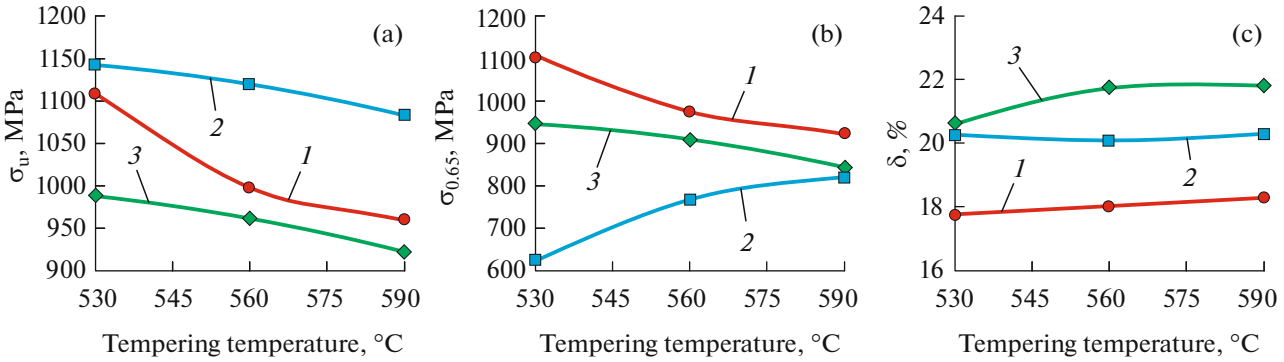

Fig. 5. Influence of tempering temperature on tensile strength (a), limit (b) and elongation (c) of steels with compositions 1–3.

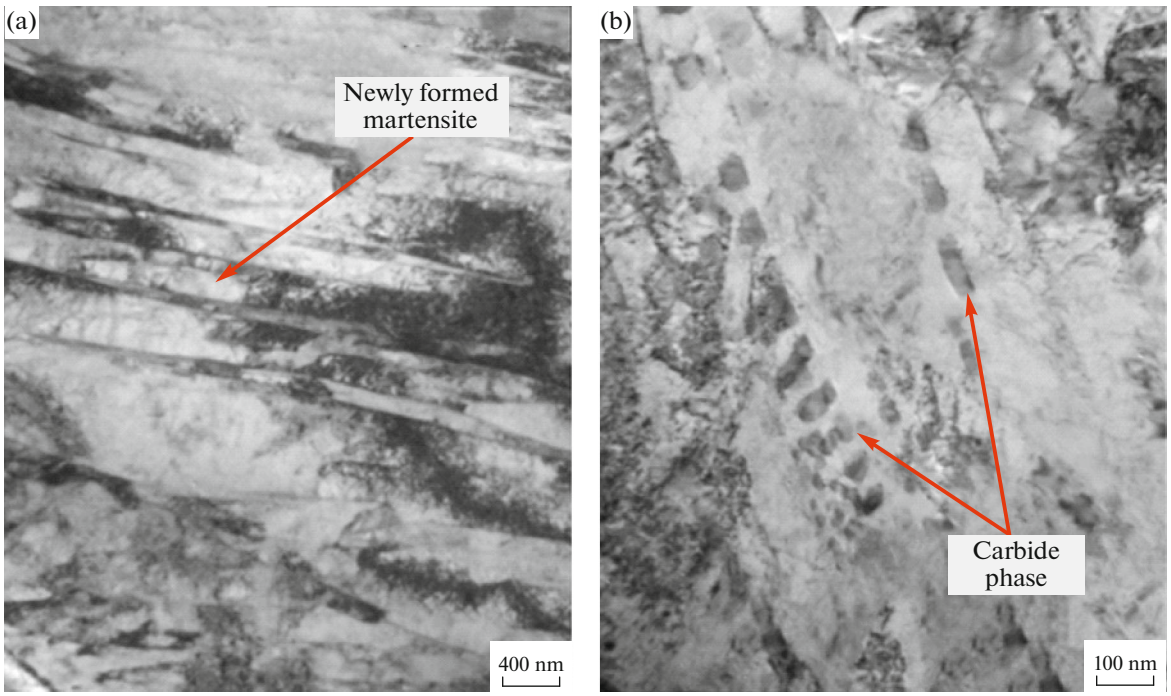

Fig. 6. Newly formed lath martensite (a) and carbides (b) in the microstructure of steel 2 after quenching at 1020°C and annealing at 760°C.

increased concentration of chromium and molybdenum (Fig. 7), which allows classifying these carbides as $Me_{23}C_6$ carbides. To achieve a set of high strength properties of austenitic martensitic steel, its annealing is followed by a final tempering at 530°C characterized by the release of dispersed carbides at the decay of *fresh* martensite as well as redistribution and reduction of dislocation densities. This leads significant increases the yield strength from 770 MPa (after annealing) to 970 MPa, while maintaining the tensile strength of at least 1070 MPa and relative elongation within 20–21%.

DISCUSSION OF RESULTS

It is known that the possibility of varying the chemical composition in martensitic stainless steels is limited to a large extent [21]. An increase in the content of chromium and other ferrite-forming elements leads to the generation of δ ferrite in the microstructure and the corresponding transition to the martensitic-ferritic steels. An increase in the total content of austenite-forming as well as ferrite-forming elements contributes to the retention of residual austenite in the microstructure with the transition to austenitic-martensitic steels. This shows an essential effect on the possibility to achieve a set of high strength and viscoplastic characteristics along with corrosion resistance.

The studies have shown that the selected steels different in composition are characterized by different temperature intervals of main transformations. The steel of basic composition 1 is a typical representative of martensitic (supermartensitic) steels. The increased chromium content in molybdenum- and tungsten-

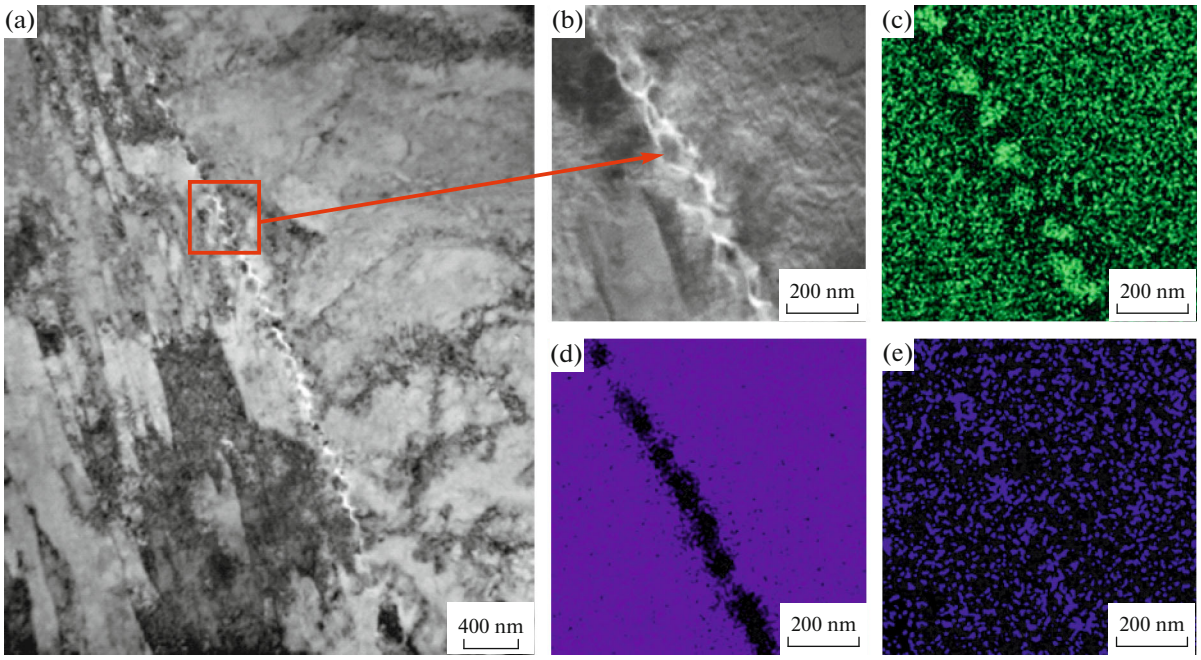

Fig. 7. Microstructure (a, b) and distribution of chemical elements (Cr (c), Fe (d), Mo (e)) in steel 2 after quenching at 1020°C and annealing at 760°C.

alloyed composition 3 steel determines the generation of a significant amount of ferrite in the microstructure along with martensite. At the same time, the higher nickel content in composition 2 steel leads to the formation of a two-phase austenitic-martensitic structure, which generally corresponds by type to semi-austenitic high-strength steels with dispersion hardening, such as UNS S15700, S14800 [22].

The estimation of the structural class of the test steels using the known empirical formulas, recommended in Appendix D of DIN EN 10088:1 [23] for stainless steels, showed a number of features (Table 3). According to the criteria of [23], the steel with basic composition 1 must be classified as martensitic ferritic since design parameter FM, determined for the position of the lines in the Schaeffler–deLong diagram is much below 1.0. That said, parameter MS_1 equal of the design initial temperature of martensitic transformation determined by the Gooch formula [24] is also lower than the range of values for martensitic steels (100–300). It should also be noted that design martensitic transformation temperatures MS_1 and MS_2 are much lower than the dilatometrically determined martensitic temperature.

The indicated design criteria do not allow correctly determining the structural class of composition 2 steel since parameter MNA <100 calculated on the basis of MD30 allows classifying this steel as metastable austenitic. That said, the initial temperatures of martensitic transformation calculated by both formulas are much lower than the empirically determined temperatures.

The estimation of the class of composition 3 steel by the minimal value of parameter FM allows classifying this steel as martensitic ferritic. The estimated initial temperatures of martensitic transformation are also very much reduced in comparison with the test data.

Thus, all of the test steels have marked differences in the estimation of their structural classes and mar-

Table 3. Estimation of structural class of the studied steels [23]

Composition	FM	MS_1	MNK	MNA	MS_2	Estimation class
1	0.68	91.50	–16.2	158.3	55.5	Martensitic ferritic
2	0.79	–8.00	–20.8	68.0	–51.0	Metastable austenitic
3	0.47	47.85	–21.1	94.1	–60.5	Martensitic ferritic

MS_1 is for martensitic and martensitic ferritic steels; MS_2 is for austenitic steel.

tensitic transformation temperatures on the basis of the relations of [23] and the totality of the conducted tests. It should be noted that the estimation by the well-known method of J.M. Potak and E.A. Sagalevich [15] provides more adequate results for the test compositions and predicts that

the fraction of δ ferrite in composition 1 steel is less than 1–2%, the fraction of austenite in

composition 2 steel is about 50%, and the fraction of δ ferrite in composition 3 steel is 30%.

Thus, the established phase composition formation patterns allow achieving pipe strength characteristics typical of groups Q125 and Q135 in accordance with GOST 31446–2017 when using composition 1 martensitic steel quenched from 960°C and subsequently tempered at temperatures from 530 to 590°C.

The amount of residual austenite in composition 2 steel with a large amount of chromium but a high nickel content can be minimized by annealing in the lower part of the austenitic region at 760°C; the technique is known as usually applied for semiaustenitic stainless steels. This process is accompanied by the release of carbides, such as $Me_{23}C_6$ and significantly broadens the martensitic transformation interval due to the depletion of austenite in carbon and carbide-forming elements [18]. In combination with the tempering at 530°C, it provides enhanced strength properties while maintaining the ductility of the material. The effect of the partial binding of chromium to carbides at this treatment on the corrosion resistance of steel requires a separate analysis.

The high-strength properties of composition 3 martensitic-ferritic steel that satisfy the requirements of Q125 strength group are produced in the mode similar to the mode used to process composition 2 steel. However, the high proportion of δ ferrite, which reaches 30% and is caused by an increased content of ferrite-forming elements, can significantly decrease the impact ductility [25, 26] and cause the development of local corrosion in the places of its accumulation.

The choice of a steel composition is determined by the possibility of obtaining a given set of properties while ensuring acceptable processing characteristics, in particular, the hot ductility of steel, which is highly dependent on the phase composition of steel at its deformation temperature. The formation of completely or mainly austenitic structures at hot pressing or rolling temperatures of 1050–1250°C is preferable. From this point of view, the most convenient materials are composition 1 and 2 steels with the maximum ratio of austenite- and ferrite-forming elements, since the calculated initial temperature of the formation of δ ferrite from austenite $T_{\gamma\to\delta}$ is rather high (1155°C). The increased content of chromium and ferrite-forming elements in composition 3 steel determines a lower temperature of $T_{\gamma\to\delta}$ (1020°C), which is less favorable, since it determines the presence of a significant amount of δ ferrite at the temperature of heating under hot deformation.

CONCLUSIONS

According to the tests, the corrosion resistance of stainless steel is hard to improve by increasing the chromium content while ensuring high strength characteristic of martensitic materials with a basic chromium content of 13% due to significant changes in the evolution of phase transformations even at low variations in the content of austenite- and ferrite-forming elements. An increase in the amount of Cr and other ferrite-forming elements determines the probability of the occurrence of δ ferrite in mostly a martensitic structure, whereas the structure retains a lot of austenite residues with an increase in the fraction of austenite-forming elements, which impedes the achievement of high-strength states. As shown by the example of composition 2 steel, the amount of austenite residues in this steel is significantly reduced by the intermediate annealing at 760°C that ensures the release of $Me_{23}C_6$ carbides, which allows having high strength after final tempering without reducing the ductility of steel.

ACKNOWLEDGMENTS

We are especially grateful to Khatkevich, V.M. and Arsenkin, A.M. from OOO TMK STC for assistance in electron microscopy analysis as well as Mikhailov, S.B. of UrFU for assistance in conducting a dilatometric study.

CONFLICT OF INTEREST

The authors declare that they have no conflicts of interest.

REFERENCES

1. Kimura, M., Tamari, T., and Shimamoto, K., High Cr stainless steel OCTG with high strength and superior corrosion resistance, *JFE GIHO*, 2005, no. 9, pp. 7–12.
2. Bellarby, J., *Well Completion Design*, Elsevier, 2009.
3. Dent, Ph.N., Evaluation of the seabed temperature corrosion and sulphide stress cracking (SSC) resistance of weldable martensitic 13% chromium stainless steel (WMSS), *Master Thesis*, Birmingham: University of Birmingham, 2014. https://etheses.bham.ac.uk/id/eprint/6871/2/Dent16MPhil.pdf. Cited October 12, 2021.
4. Ishiguro, Y., Suzuki, T., Eguchi, K., Nakahashi, T., and Sato, H., Martensite-based stainless steel OCTG of 15Cr-based and 17Cr-based material for sweet and mild sour condition, *European Corrosion Congress*, 2014.
5. Jiang, W., Zhao, K., Ye, D., and Li, J., Effect of heat treatment on reversed austenite in Cr15 super martensitic stainless steel, *J. Iron Steel Res. Int.*, 2013, vol. 20, no. 5, pp. 61–65. https://doi.org/10.1016/S1006-706X(13)60099-0
6. Jiang, W., Zhao, K., Liu, X., Zhou, Y.H., Ye, D., Su, J., and Yong, Q., The influence of heat treatment on microstructure and mechanical properties of Cr15 super

martensitic stainless steel, *Adv. Mater. Res.*, 2012, vols. 393–395, pp. 440–443. https://doi.org/10.4028/www.scientific.net/AMR.393-395.440

7. Tsai, W.-J. and Lin, C.-K., Corrosion fatigue behaviour of 15Cr–6Ni precipitation-hardening stainless steel in different tempers, *Fatigue Fract. Eng. Mater. Struct.*, 2008, vol. 23, n. 6, pp. 489–497. https://doi.org/10.1046/j.1460-2695.2000.00313.x
8. Mariani, F.E., Takeya, G.S., Casteletti, L.C., Lombardi, A.N., and Totten, G.E., Heat treatment of precipitation-hardening stainless steels alloyed with niobium, *Mater. Perform. Charact.*, 2016, vol. 5, no. 1, pp. 38–46. https://doi.org/10.1520/MPC20150039
9. Wang, Z., Li, H., Shen, Q., Liu, W., and Zhanyong, W., Nano-precipitates evolution and their effects on mechanical properties of 17-4 precipitation-hardening stainless steel, *Acta Mater.*, 2018, vol. 156, pp. 158–171. https://doi.org/10.1016/j.actamat.2018.06.031
10. Prabowo, H., Pratesa, Y., Munir, B., Ulum, R., and Wahyuadi, J., Preliminary assessment of 22Cr and 15Cr materials selection for CO_2 enhanced oil recovery program, *MATEC Web Conf.*, 2019, vol. 269, p. 03014. https://doi.org/10.1051/matecconf/201926903014
11. Pumpyansky, D.A., Pyshmintsev, I.Yu., Bityukov, S.M., Alieva, E.S., Gusev, A.A., Mikhailov, S.B., and Lobanov, M.L., Features of phase transformations in martensitic steel for high-strength corrosion-resistant pipes, *Metallurgist*, 2022, vol. 65, nos. 11–12, pp. 1245–1254. https://doi.org/10.1007/s11015-022-01270-w
12. Alekseev, V.I., Yusupov, V.S., and Lazarenko, G.Yu., Mechanism of influence of molybdenum and copper on anticorrosion properties of steel, *Perspektivnye Mater.*, 2009, no. 6, pp. 21–29.
13. Chenna, KrishnaS., Pant, B., Jha, A., George, K.M., and Gangwar, N.K., Microstructure and properties of 15Cr5Ni1Mo1W martensitic stainless steel, *Steel Res. Int.*, 2015, no. 86, no. 1, pp. 51–58. https://doi.org/10.1002/srin.201400035
14. Kumar, A.V., Gupta, R.K., Amruth, M., Ramkumar, P., and Narahari, P., Development and characterization of 15Cr5Ni1W martensitic precipitation hardening stainless steel for aerospace applications, *Mater. Sci. Forum*, 2015, vols. 830–831, pp. 15–18. https://doi.org/10.4028/www.scientific.net/MSF.830-831.15
15. Potak, Ya.M., *Vysokoprochnye stali* (High-Strength Steels), Moscow: Metallurgiya, 1972.
16. Thermo-Calc. https://thermocalc.com/products/thermo-calc. Cited April 11, 2020.
17. *Med' v chernykh splavakh. Sbornik statei* (Copper in Ferrous Metals: Coll. of Papers), Le Mei, I. and Shetka, L.M.-D., Eds., Moscow: Metallurgiya, 1988.
18. Pickering, F.B., *Physical Metallurgy and the Design of Steels*, Applied Science Publishers, 1978.
19. Tarasenko, L.V. and Unchikova, M.V., Effect of double aging on mechanical and corrosion properties of maraging steel 06Cr14Ni6Cu-2MoNbTi, *Vestn. Mosk. Gos. Tekh. Univ. im. N.E. Baumana. Ser. Mashinostr.*, 2014, no. 4, pp. 123–130.
20. Tarasenko, L.V. and Unchikova, M.V., Heat treatment of corrosion-resistant steel for manufacture of force-measuring elastic elements, *Vestn. Mosk. Gos. Tekh. Univ. im. N.E. Baumana. Ser. Mashinostr.*, 2007, no. 2, pp. 82–88.
21. ASM HANDBOOK. Properties and Selection: *Irons, Steels, and High-Performance Alloys, ASM International*, 1990, vol. 1. https://doi.org/10.31399/asm.hb.v01.9781627081610
22. *ASM Specialty Handbook: Stainless Steels*, Davis, J.R., Ed., ASM International, 1994.
23. *DIN EN 10088:1-2014: Stainless steels—Part 1: List of stainless steels*, 2014.
24. Gooch, T., Welding martensitic stainless steels, *Weld. Inst. Res. Bull.*, 1977, no. 18, pp. 343–349.
25. Hu, X., Luo, X., Xiao, N., and Li, D., Effects of δ-ferrite on the microstructure and mechanical properties in a tungsten-alloyed 10% Cr ultrasupercritical steel, *Acta Metall. Sin.*, 2009, vol. 45, no. 5, pp. 553–558.
26. Korneev, A.E., Gromov, A.F., and Kiselev, A.M., Effect of δ-ferrite on the properties of martensitic steels, *Met. Sci. Heat Treat.*, 2013, vol. 55, nos. 7–8, pp. 445–450. https://doi.org/10.1007/s11041-013-9652-2

Translated by S. Kuznetsov